

Observation of Thermopower Oscillations in the Coulomb Blockade Regime in a Semiconducting Carbon Nanotube

M. C. Llaguno, J. E. Fischer, and A. T. Johnson, Jr.*

Department of Physics and Astronomy and Laboratory for Research on the Structure of Matter, University of Pennsylvania, Philadelphia, Pennsylvania 19104

J. Hone

Department of Mechanical Engineering, Columbia University, New York, New York 10027

Received October 1, 2003; Revised Manuscript Received November 2, 2003

ABSTRACT

We have measured the thermoelectric power (TEP) and Coulomb charging characteristics of an individual p-type semiconducting single-wall carbon nanotube (SWNT) in the quantum dot regime. The TEP measured as a function of gate voltage oscillates around a baseline value that is first positive and becomes more negative as the SWNT is depleted. When the device behaves as a single quantum dot, the TEP oscillation period and amplitude agree with theory. We ascribe the positive baseline level to p-type Schottky barriers at the SWNT–metal contacts, and the negative baseline to n-type barrier regions that cause multidot behavior as carriers are removed from the system. Near depletion, large TEP oscillations are observed even though Coulomb oscillations of the conductance are immeasurably small.

Several reasons motivate careful investigation of the thermoelectric power (TEP; $S = -\Delta V/\Delta T$) of individual single-wall carbon nanotubes (SWNTs). First, TEP is a basic electronic response function of a material: its sign reflects that of the majority carriers and the temperature dependence can be used to elucidate the conduction mechanism¹ and interaction with lattice vibrations.² Despite intense interest in electrical and thermal transport in nanotubes, measurement of the TEP of individual SWNTs has not yet been reported. Second, TEP of bulk SWNT material³ shows marked response to chemical doping,⁴ pressure,⁵ and gas exposure.^{6,7} The data remain poorly understood, especially the relative contributions of semiconducting tubes, metallic tubes, and junctions between tubes. Therefore, measurement of the TEP of individual nanotubes will inform the development of proposed SWNT-based gas detectors, where both conductance and thermopower are used as signals. Third, one-dimensional (1-D) materials are thought to be ideal for thermoelectric applications,⁸ so tools for direct measurement of individual 1-D nanostructures are highly desirable. Finally, nanotubes can be used as a model system to study thermoelectric effects in low-dimensional systems such as quantum dots. Here we report first results from our work in this

direction: the TEP of an individual semiconducting SWNT quantum dot. Along with addressing the important issues listed above, we also find that the TEP oscillations are a highly sensitive probe of on-tube defects.

Several basic properties of the TEP are important for the discussion of the experiment. For a semiconductor, the TEP diverges as $S(T) \sim (E_g - \mu)/2eT$, where E_g is the energy of the band edge, and μ the chemical potential. In the Coulomb blockade regime, theory predicts⁹ that the charging energy plays a role similar to the semiconductor band gap. The TEP of a metallic quantum dot with total capacitance C oscillates about zero in a sawtooth fashion as a function of gate voltage with a peak-to-peak amplitude of $E_C/2eT$, where $E_C = e^2/C$ is the charging energy. The period of the TEP oscillations is predicted to be equal to that of the Coulomb oscillations in the conductance.

The thermopower of quantum dots has been studied experimentally^{10,11} in quantum dots defined from two-dimensional electron gas, but comparison to theory is complicated since the temperature gradient applied to the buried electron gas is inferred rather than measured directly. The temperature gradient across a SWNT quantum dot, on the other hand, can be measured directly, because a SWNT QD can be quite long ($\sim 1 \mu\text{m}$) and enters the Coulomb

* Corresponding author. E-mail: cjohnson@physics.upenn.edu

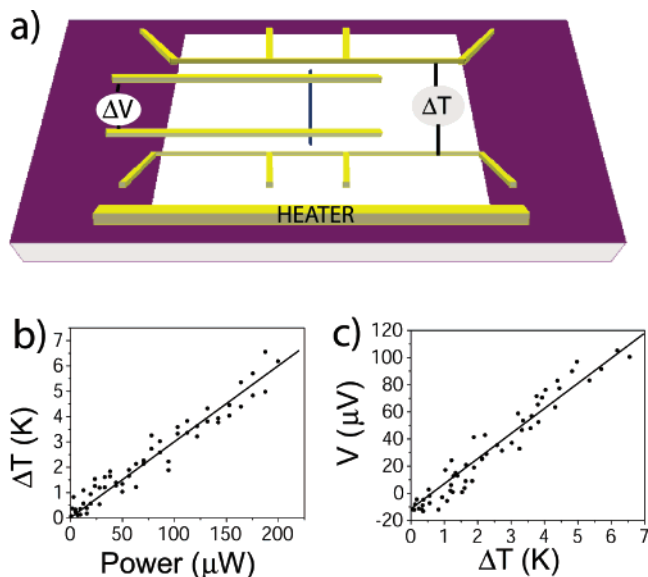


Figure 1. (a) Device schematic. A heater is near one end of the tube and extends across the entire membrane to provide a uniform temperature gradient. (b) Measured temperature difference across the sample as a function of heater power. (c) The measured TEP is proportional to the temperature difference.

blockade regime at relatively high temperature (5–50 K, as opposed to less than 1 K for typical 2DEG quantum dots) where electrons are still thermally well-coupled to the lattice. The temperature dependence of the TEP of a single multiwall nanotube has been reported, but the device did not exhibit the quantum dot behavior that is the focus of this work.¹²

Figure 1a shows the sample geometry used for this experiment. SWNTs are grown by chemical vapor deposition (CVD)^{13–15} on a free-standing silicon nitride membrane for enhanced thermal isolation.¹⁶ Electron-beam lithography is used to define two voltage probes attached to the ends of the tube, two thin-film thermometers in a four-probe configuration, and a large heater wire at one side of the device. The sample used for this experiment had radius $r = 1$ nm as measured by atomic force microscopy (AFM). The distance between the contacts was $L = 4.4$ μm . From the AFM-measured diameter, we estimate the SWNT band gap to be 400 meV.¹⁷ Measurements are conducted at 6 K in a vacuum in a liquid helium cryostat. To calibrate the thin-film thermometers, their 4-probe resistance is measured as the cryostat is cooled slowly to its base temperature.

Care is taken to ensure that the temperature gradient between the heater and the low-temperature bath on the opposite side of the membrane is uniform so the temperature difference across the SWNT can be estimated reliably. The heater wire is wide (50 μm) compared to the SWNT diameter, and it is located far (20 μm) from the SWNT device compared to the SWNT length, so heat flows uniformly as it nears the device region. Although SWNT thermal conductivity is very high at room temperature (> 1000 W/m-K), it decreases roughly linearly with temperature. At the measurement temperature of 6 K, it is roughly 20 W/m-K,¹⁸ close to that of the SiN membrane (1–3 W/m-K).¹⁹ Since the membrane is much thicker than the SWNT cross section (100 nm compared to 0.3 nm), the thermal conductance of

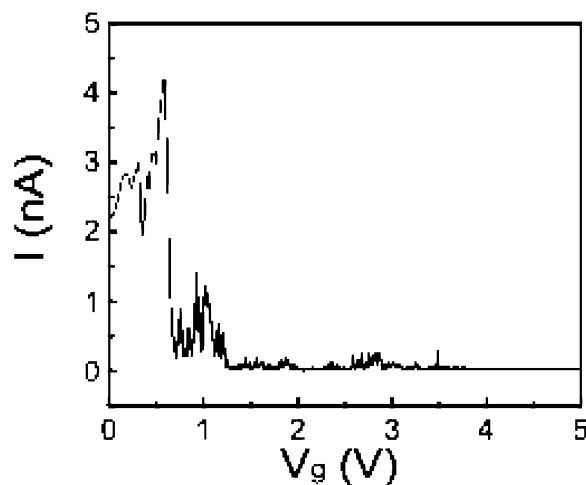


Figure 2. Current through the device as a function of the backgate voltage. The bias voltage is 10 mV and the temperature is 6 K.

the membrane directly beneath the SWNT is comparable to or greater than that of the SWNT itself. The heat flow in the device region thus is uniform and not strongly perturbed by the SWNT. This conclusion holds for any gate voltage, since the thermal conduction of SWNTs is dominated by phonons. At 6 K we expect strong thermal coupling between the SWNT and the substrate beneath it as well as between the SWNT electrons and phonons.

The TEP of the nanotube is measured as follows. First, the temperature difference between the thin film thermometers is measured as a function of heater power (Figure 1b). The temperature difference ΔT across the SWNT is then inferred from the measured temperature difference between the thermometers: as justified above, the temperature gradient is uniform. To measure the TEP, the voltage ΔV across the tube is measured as a function of ΔT . The raw data show the expected linear relationship (Figure 1c). The TEP is measured as a function of gate voltage V_g by repeating the ΔV vs ΔT measurement as V_g is stepped. We omit the very small (< 1 $\mu\text{V/K}$) correction for the TEP of the gold leads at 6 K. Coulomb and TEP oscillations are measured during separate gate voltage sweeps.

Figure 2 shows the current, I , carried by the device as a function of gate voltage in the range $0 < V_g < 5$ V. Overall, I decreases with increasing V_g and becomes negligible (less than 10 pA) above $V_g = 4$ V. This is consistent with the well-studied behavior of the semiconducting nanotube field effect transistor (TubeFET), with p-type behavior due to exposure to atmosphere. Superimposed on this behavior are Coulomb oscillations of the current that reflect single-electron charging (Coulomb blockade) effects. The period of the Coulomb oscillations is not constant, as would be expected for an ideal metallic quantum dot, but changes with V_g . The Coulomb oscillation behavior falls roughly into three categories for different gate voltage ranges; each range of V_g shows a distinct behavior in the measured TEP as well. As discussed in detail below, there is a single quantum dot regime for $V_g < 0.65$ V, a regime with multiple quantum dots along the SWNT length at intermediate V_g ($0.8 < V_g < 1$ V), and finally a very low conduction (below the

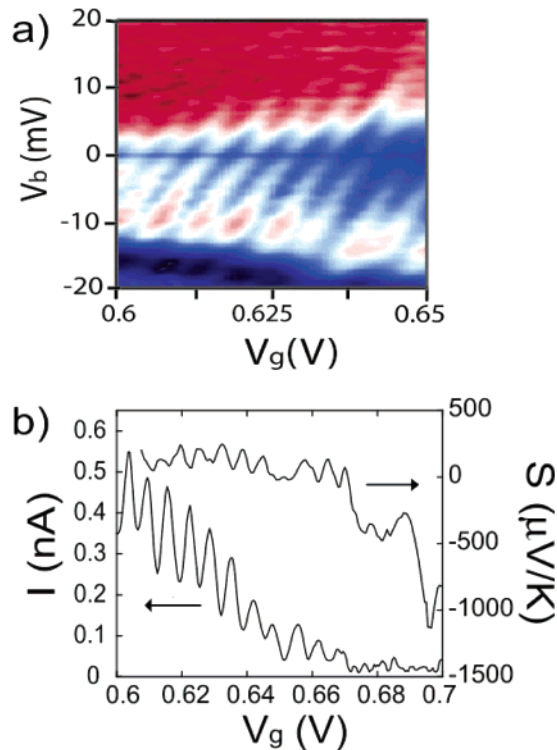


Figure 3. (a) Color scale representation of the differential conductance (dI/dV_b) as a function of source–drain bias voltage (V_b) and gate voltage (V_g) in the single quantum dot regime. dI/dV_b increases as the color ranges black to blue to red to white. (b) Current and TEP as a function of gate voltage. The TEP oscillates around a small positive baseline level with the same periodicity as the Coulomb oscillations of the current. For the conductance measurement, the bias voltage is 2 mV. All data were taken at $T = 6$ K.

measurement sensitivity of 1 nS) regime for $V_g > 4.3$ V as the sample approaches depletion.

Figure 3a shows the charging spectrum of the nanotube in the range $0.6 < V_g < 0.65$ V. The presence of a regular charging diamond structure in this region (gate voltage period near 6 mV) indicates that the nanotube acts as a single quantum dot in the Coulomb blockade regime. Figure 3b shows that the TEP oscillates as a function of gate voltage with a nearly identical period, exactly as predicted by theory for TEP in the Coulomb blockade regime. Both data sets are reproducible but since Coulomb and TEP oscillations are taken in separate V_g sweeps (see above), random motion of trapped charge near the nanotube leads to slight deviations in the oscillation period and phase. The TEP oscillations are small ($\sim 150 \mu\text{V/K}$ peak-to-peak) and centered on $+100 \mu\text{V/K}$ for $V_g < 0.68$ V.

In the intermediate range (Figures 4a,b), the Coulomb oscillation period increases to approximately 10 mV, and the charging spectrum shows a periodic modulation, reflecting the formation of multiple quantum dots in series.²⁰ The TEP oscillations display the same period and modulation as the Coulomb oscillations of the current (Figure 4b), are large ($\sim 500\text{--}700 \mu\text{V/K}$ peak-to-peak), and are centered on a negative value (roughly $-500 \mu\text{V/K}$). At high gate voltages ($V_g > 4.3$ V), the device current is immeasurably small at

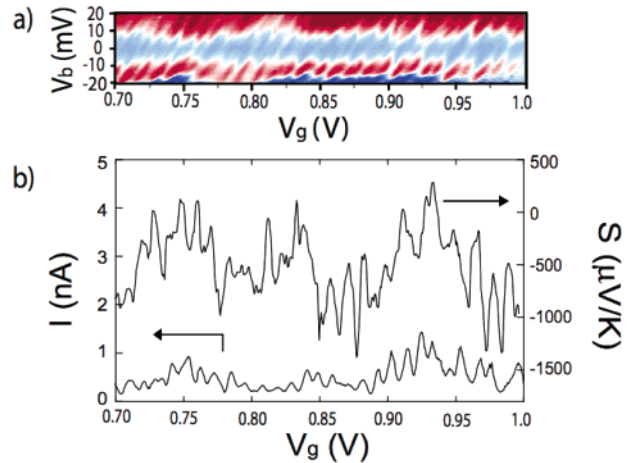


Figure 4. (a) dI/dV_b plotted in a color scale as a function of (V_g , V_b). dI/dV_b increases as the color evolves from black to blue to red to white. Modulation of the diamond heights indicates multidot behavior. (b) Device current and TEP as a function of gate voltage. For the current measurement, the bias voltage is 10 mV. The TEP oscillations are much larger than in Figure 3 and the baseline level is negative. All data were taken at $T = 6$ K.

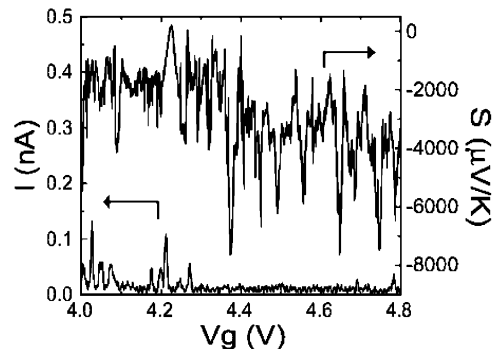


Figure 5. Device current and TEP as a function of gate voltage in the near-depletion regime. For the conductance measurement, the bias voltage is 20 mV. The TEP oscillations are very large and the baseline level is large and negative. All data were taken at $T = 6$ K.

low-bias (Figure 5). The TEP, however, oscillates very sharply ($\sim 2000\text{--}4000 \mu\text{V/K}$ peak-to-peak) around sizable negative values ($\sim -3000 \mu\text{V/K}$) with a large and irregular period.

The TEP data described above show two distinct features. First, the TEP oscillates; the oscillation period matches that of the Coulomb oscillations of the current (when the latter are observable), and its amplitude increases with increasing gate voltage. Second, the TEP oscillations are not centered on zero, but instead around a baseline value whose sign and magnitude change with V_g . We attribute the TEP oscillations to single electron charging and the baseline TEP level to barriers associated with energy band fluctuations within the device. For $V_g < 0.65$ V, the baseline is positive and ascribed to Schottky barriers known to form at metal contacts to semiconducting SWNTs.¹⁵ For $V_g > 0.65$ V, the baseline becomes negative. We suggest a model where n-type semiconducting barrier regions form along the length of the SWNT as the valence band is depleted (see Figure 6).²⁰ These

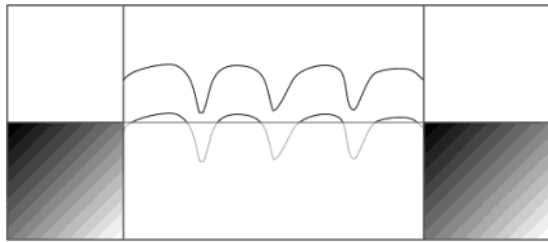


Figure 6. Schematic of the proposed SWNT energy band structure in the multidot regime. Barriers that form along the nanotube length are n-type and contribute a negative thermopower.

barrier regions, presumably associated with defects and/or adsorbates,²¹ break the tube into separate conducting regions, resulting in the observed multidot behavior. We first consider the oscillatory component of the TEP, then turn to the background level in the following paragraph.

In the first two regimes described above, the measured TEP oscillations have the same period as Coulomb oscillations of the current, as predicted by theory for TEP in the charging regime.⁹ The amplitude of the TEP oscillations also agrees well with theoretical predictions. For $V_g < 0.65$ V (Figure 3a), the size of the diamonds in the charging spectrum data give $E_C = 2$ meV. This is in reasonable agreement with the value of 1 meV calculated taking the capacitance of the cylindrical SWNT to the backgate to be $C = 2\pi\epsilon L/\ln(2h/r)$, where $\epsilon = 4$ is the average dielectric constant of silicon nitride and vacuum, $L = 4.4$ μm the nanotube length, $h = 100$ nm the gate dielectric thickness, and $r = 1$ nm the nanotube radius. Theory predicts a peak-to-peak TEP oscillation amplitude of $E_C/2(6\text{ K}) \sim 170$ $\mu\text{V/K}$, close to the observed value of 150 $\mu\text{V/K}$. In the intermediate range ($0.8 < V_g < 1$ V, Figure 4a), the measured E_C increases to about 10 meV. This is consistent with the formation of two quantum dots in series along the tube; the measured E_C is the sum of the dot charging energies. The expected peak-to-peak variation in the TEP is now 0.8–1.1 mV/K, slightly larger than the 500–700 $\mu\text{V/K}$ observed. This is consistent with multiple dot formation, because each quantum dot within the nanotube will experience only a fraction of the total temperature drop between the contacts.

Near full depletion ($V_g > 4.3$ V), TEP provides us with information about the device that is *not* available from the measured conductance. No visible Coulomb oscillations appear in the conductance but the TEP continues to oscillate, indicating that sections of the nanotube continue to conduct and add single electrons (i.e., they are not fully depleted of carriers) but large barriers suppress electron transport below the measurement sensitivity. The TEP oscillation is very large (~ 3000 $\mu\text{V/K}$), as expected since the quantum dot (non-depleted) portion of the nanotube is short, with a large associated charging energy. This TEP oscillation size corresponds to conducting nanotube segments about 100 nm long. Thus the TEP is a useful probe of localized states that carry negligible transport current.

We now consider the observed variation in the baseline TEP, around which the TEP oscillations occur. For $V_g <$

0.65 V, this value is about +100 $\mu\text{V/K}$. Schottky barriers at the tube–metal contact have been measured to have a height of $\Delta = 150$ meV^{15,22} and should have a TEP of $\Delta/2eT$, appropriate for a p-type semiconductor. The temperature difference across the Schottky barriers will be proportional to their length \mathcal{L} , resulting in a TEP given by $S = (\Delta/2eT)(\mathcal{L}/L)$. The measured TEP baseline of 100 $\mu\text{V/K}$ thus corresponds to combined length of 35 nm for the two Schottky barriers. This value is reasonable given the measured barrier transmission in this range of V_g , $T = Gh/4e^2 \sim 0.002$.

As the gate voltage increases, the TEP baseline becomes progressively more negative. We associate this with the formation of n-type barriers along the length of the semiconducting nanotube as it becomes depleted. At first these barriers break the tube into multiple quantum dots (for $V_g > 0.7$ V), and eventually they suppress conduction completely. If we consider the tube as a bulk semiconductor, we can estimate an average energy difference between the Fermi level μ and the conduction band edge E_g when the nanotube is significantly depleted ($V_g > 4.6$ V). We use the formula for the TEP of a bulk semiconductor, $S = -(E_g - \mu)/2eT$, and the measured TEP baseline of approximately -5 meV/K to find an average value $E_g - \mu \sim 30$ meV. This is reasonable given the estimated band gap of 400 meV for the sample, which requires the energy difference to be less than 200 meV. If we assume that this averaged energy band offset is also characteristic of the barriers present in the intermediate regime ($0.8 < V_g < 1$ V), the measured TEP offset of roughly -500 $\mu\text{V/K}$ implies that roughly 10% of the tube length, or 400 nm, consists of barrier regions.

In summary, we have developed a device for measuring the thermopower of individual carbon nanotubes and have measured $S(V_g)$ of a semiconducting nanotube in the Coulomb blockade regime. The TEP shows distinct oscillations around a nonzero baseline value that becomes more negative as the nanotube is depleted. In the regime where the nanotube acts as a single quantum dot, both the TEP oscillation period and peak-to-peak oscillation size are in semiquantitative agreement with theory. The measured TEP is used to infer properties of defects and localized states along the SWNT as it is depleted. TEP oscillations reveal the presence of single charge depletion even at gate voltages where Coulomb oscillations are immeasurably small and are used to estimate the length of residual conducting regions within the nanotube. We use the measured positive TEP baseline to determine that p-type Schottky barriers at the nanotube contacts have a total length of 35 nm when the nanotube is in the single quantum dot regime. A negative TEP offset appears when the nanotube enters the multi-quantum dot regime due to the formation of n-type barrier regions along the tube length. These results, along with the outcome of further experiments of this type, will benefit understanding and eventual engineering of SWNT-based devices and sensors.

Note: During the preparation of this manuscript, we became aware of related work with similar conclusions from Joshua P. Small et al.

Acknowledgment. This work was supported by the National Science Foundation NIRT (PHY-0103552), the Petroleum Research Fund, and the U.S. Department of Energy Grant No. DE-FG02-98ER45701 (M.C.L., J.E.F.).

References

- (1) Chaikin, P. M. In *Organic Superconductivity*; Kresin, V. Z., Little, W. A., Eds.; Plenum Press: New York, 1990; pp 101–115.
- (2) Vavro, J.; Llaguno, M. C.; Fischer, J. E.; Ramesh, S.; Saini, R. K.; Ericson, L. M.; Davis, V. A.; Hauge, R. H.; Pasquali, M.; Smalley, R. E. *Phys. Rev. Lett.* **2003**, *90*, 065503.
- (3) Hone, J.; Ellwood, I.; Muno, M.; Mizel, A.; Cohen, M. L.; Zettl, A.; Rinzler, A. G.; Smalley, R. E. *Phys. Rev. Lett.* **1998**, *80*, 1042–1045.
- (4) Grigorian, L.; Sumanasekera, G. U.; Loper, A. L.; Fang, S.; Allen, J. L.; Eklund, P. C. *Phys. Rev. B* **1998**, *58*, R4195–R4198.
- (5) Barisic, N.; Gaal, R.; Kezsmarki, I.; Mihaly, G.; Forro, L. *Phys. Rev. B* **2002**, *65*, 241403.
- (6) Collins, P. G.; Bradley, K.; Ishigami, M.; Zettl, A. *Science* **2000**, *287*, 1801–1804.
- (7) Sumanasekera, G. U.; Adu, C. K. W.; Fang, S.; Eklund, P. C. *Phys. Rev. Lett.* **2000**, *85*, 1096–1099.
- (8) Dresselhaus, M. S.; Dresselhaus, G.; Sun, X.; Zhang, Z.; Cronin, S. B.; Koga, T.; Ying, J. Y.; Chen, G. *Microscale Therm. Eng.* **1999**, *3*, 89–100.
- (9) Beenakker, C. W. J.; Staring, A. A. M. *Phys. Rev. B* **1992**, *46*, 9667–9676.
- (10) Staring, A. A. M.; Molenkamp, L. W.; Alphenaar, B. W.; Vanhouten, H.; Buyk, O. J. A.; Mabesoone, M. A. A.; Beenakker, C. W. J.; Foxon, C. T. *Europhys. Lett.* **1993**, *22*, 57–62.
- (11) Dzurak, A. S.; Smith, C. G.; Pepper, M.; Ritchie, D. A.; Frost, J. E. F.; Jones, G. A. C.; Hasko, D. G. *Solid State Commun.* **1993**, *87*, 1145–1149.
- (12) Kim, P.; Shi, L.; Majumdar, A.; McEuen, P. L. *Phys. Rev. Lett.* **2001**, *87*, art. no.-215502.
- (13) Hafner, J. H.; Cheung, C. L.; Oosterkamp, T. H.; Lieber, C. M. *J. Phys. Chem. B* **2001**, *105*, 743–746.
- (14) Kim, W.; Choi, H. C.; Shim, M.; Li, Y. M.; Wang, D. W.; Dai, H. *J. Nano Lett.* **2002**, *2*, 703–708.
- (15) Freitag, M.; Radosavljevic, M.; Zhou, Y. X.; Johnson, A. T.; Smith, W. F. *Appl. Phys. Lett.* **2001**, *79*, 3326–3328.
- (16) We use double-side polished <100> silicon wafers with $h = 100$ nm of low-stress silicon nitride deposited on each side. (UC Berkeley Microfabrication Laboratory). Specific regions of the silicon substrate are removed using photolithography and anisotropic etching in an aqueous KOH solution to leave suspended silicon nitride membranes $80 \mu\text{m}$ on a side. The membrane is coated with a 20 nm silicon monoxide buffer layer, and SWNTs are then grown by catalytic chemical vapor deposition (CVD) at 950°C using an iron(III) nitrate solution (50 mg in 1 L 2-propanol) as the catalyst source and a mixture of ethylene and methane (5 and 3000 sccm, respectively) as the feedstock gas. SWNTs for measurement are located by AFM. All metallic leads consist of 50 nm Au with a 5 nm Cr adhesion layer. Finally, 10 nm of gold is deposited on the back of the membrane as a gate electrode.
- (17) Saito, R.; Fujita, M.; Dresselhaus, G.; Dresselhaus, M. S. *Appl. Phys. Lett.* **1992**, *60*, 2204–2206.
- (18) Hone, J.; Llaguno, M. C.; Nemes, N. M.; Johnson, A. T.; Fischer, J. E.; Walters, D. A.; Casavant, M. J.; Schmidt, J.; Smalley, R. E. *Appl. Phys. Lett.* **2000**, *77*, 666–668.
- (19) Revaz, B.; Zink, B. L.; O’Neil, D.; Hull, L.; Hellman, F. *Rev. Sci. Instrum.* **2003**, *74*, 4389–4403.
- (20) McEuen, P. L.; Bockrath, M.; Cobden, D. H.; Yoon, Y. G.; Louie, S. G. *Phys. Rev. Lett.* **1999**, *83*, 5098–5101.
- (21) Freitag, M.; Johnson, A. T.; Kalinin, S. V.; Bonnell, D. A. *Phys. Rev. Lett.* **2002**, *89*, 216801.
- (22) Fuhrer, M. S.; Nygard, J.; Shih, L.; Forero, M.; Yoon, Y. G.; Mazzone, M. S. C.; Choi, H. J.; Ihm, J.; Louie, S. G.; Zettl, A.; McEuen, P. L. *Science* **2000**, *288*, 494–497.

NL0348488